PHOTOSYNTHETICA 39 (3) : 419-425, 2001

Multi-phasic kinetics of $P700^+$ dark re-reduction in *Nicotiana tabacum*

Ming-Xian JIN*, Zheng-Ju YAO, and Hualing MI

Shanghai Institute of Plant Physiology and Ecology, Shanghai Institutes for Biological Sciences, Chinese Academy of Sciences, 300 Fenglin Road, Shanghai 200032, China

Abstract

Reduction kinetics of $P700^+$ after far-red radiation (FR)-induced oxidation in intact tobacco leaves was examined by analysing the post-irradiation relaxation of 810-830 nm absorbance difference. The reduction curve could be de-convoluted distinctively into two or three exponential decaying components, depending on the FR irradiance, the treating and measuring temperatures, and the extent of dark adaptation. The multi-phasic kinetics of $P700^+$ re-reduction upon the turning off of FR irradiation is related to the heterogeneity of electron transport around photosystem 1 in thylakoid membranes.

Additional key words: far-red radiation; photosystem 1; tobacco.

Introduction

Photosynthetic energy conversion involves the co-operation of photosystem 1 (PS1) and photosystem 2 (PS2). In contrast to PS2, PS1 can be driven by FR in the range of 700-730 nm, and the redox state of its reaction centre, P700, can be monitored by absorption changes around 820 nm (Harbinson and Woodward 1987, Schreiber *et al.* 1988). Recently, the signal quality has been improved by application of the dual wavelength method (Klughammer and Schreiber 1998). The kinetics of P700 photoconversion under weak continuous actinic irradiation helps to understand the mechanism of electron transport around PS1. Due to its high sensitivity, non-invasiveness, and simplicity of measurement, radiant energy-induced absorbance change around 820 nm has been used as a powerful probe for PS1 functioning (Klughammer and Schreiber 1991, 1998).

Using semi-log plots of 820 nm absorbance change *versus* time, Bukhov *et al.* (1999) found that in spinach leaves the reduction of $P700^+$ after FR-irradiation was composed of two first-order kinetic components. In the present study using intact tobacco leaves, reduction kinetics of $P700^+$ was analysed as a sum of two or three exponential components, and all the kinetic parameters were fitted directly to the experimental decay curves of 810-830 nm absorbance difference by a non-linear algorithm. The effects of dark-adaptation, FR irradiance, and high temperature were also investigated.

Materials and methods

Plants of tobacco (*Nicotiana tabacum* L.) were grown on vermiculite in plastic pots in a phytotron under controlled temperature (25 °C), irradiance [200 μmol(photon) m^{-2} s^{-1}, 14 h per day], and air humidity (40 %), and irrigated with Hoagland solution. Five weeks after germination, when the seedlings reached the 7-leaf stage, P700 oxidation was measured on the youngest fully expanded leaves.

Received 27 March 2001, *accepted* 16 July 2001.
Fax: 86-21-64042385; e-mail: jin@iris.sipp.ac.cn
Abbreviations: FNR – ferredoxin-$NADP^+$ reductase; FQR – ferredoxin-plastoquinone reductase; FR – far-red radiation; LHC – light-harvesting complex; NDH – NAD(P)H-dehydrogenase; PS – photosystem.
Acknowledgement: This work was supported by the National Natural Science Foundation of China (Grant No. 39870049) and the State Key Basic Research and Development Plan (Grant No. 1998010100). We thank Prof. Tian-Duo Wang and Prof. Yun-Kang Shen for their review of the manuscript, Associate Prof. Ji-Yu Ye for his help, and the anonymous referees for their useful suggestions.

Oxidation of P700 was monitored by absorbance difference of 810 nm *minus* 830 nm, using a new dual wavelength emitter detector unit *ED-P700DW-E* combined with a standard chlorophyll fluorometer (*PAM 101*, *Walz*, Effelrich, Germany). Far-red radiation (>720 nm) for exciting PS1 was provided by a *RG720* filter (*Schott*, Mainz, Germany). Unless indicated otherwise, the far-red irradiance was 7.3 μmol(photon) m^{-2} s^{-1}. Power switch of the FR was connected with a magnetic relay controlled by a computer. The output from the *PAM 101* unit was transferred to an analogue-digital converter attached to the computer. The sampling frequency was 20 Hz. Before measurement, the leaf samples were irradiated with actinic "white light" [halogen lamp, 1000 μmol(photon) m^{-2} s^{-1}] and subsequently dark-adapted. The scheme of irradiation and data acquisition was programmed and conducted automatically. The abaxial side of the leaf under study was pressed on a thermostatted glass platform covered by a piece of black cotton cloth, and the adaxial side of the leaf was placed facing the detector encircled by a piece of plastic foam. Measurements were performed at room temperature (27 °C) unless stated otherwise.

Data analysis: The records of 810-830 nm absorbance difference were analysed using special-purpose software designed by the author. The decay kinetics of the absorbance difference, $A(t)$, upon the turning off of FR was described by a sum of discrete exponential components with amplitudes a_i and lifetimes τ_i, *i.e.*,

$$A(t) = a_0 + \Sigma a_i \exp(-t/\tau_i) \qquad (1)$$

where a_0 is a constant depending on the vertical origin. The point immediately after the turning off of FR was excluded so as to eliminate the possible artefact caused by the light tail of the actinic lamp (Jin *et al.* 2000). The horizontal origin was shifted arbitrarily to the point 0.05 s after the turning off of the lamp. The selected values were fitted to Eq. 1 by a non-linear Levenberg-Marquardt algorithm (Marquardt 1963). Starting values of the parameters were given randomly within a predefined domain. The diminishment of χ^2 values and plots of the weighted residuals evaluated the quality of fit.

Results

Typical examples of the change in 810-830 nm absorbance difference induced by FR irradiation are in Fig. 1 where the tobacco leaf had been dark-adapted for different periods. Far-red radiation (>720 nm) used in

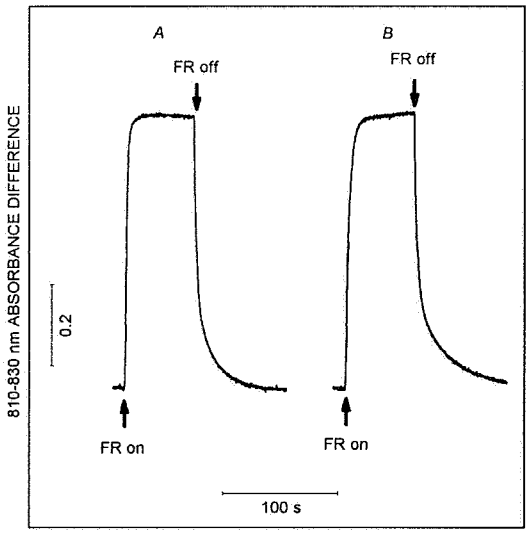

Fig. 1. Redox kinetics of P700 induced by far-red radiation [FR, 720 nm, 7.3 μmol(photon) m^{-2} s^{-1}] in intact tobacco leaf. The redox state of P700 was determined by the 810-830 nm absorbance difference. The leaf had been irradiated [halogen lamp, 1 000 μmol(photon) m^{-2} s^{-1}] for 15 min and dark-adapted for 24 min (*A*) or 3.31 h (*B*). The relaxation kinetics of the absorbance difference in *A* and *B* were expanded and analysed in Figs. 2 and 3, respectively.

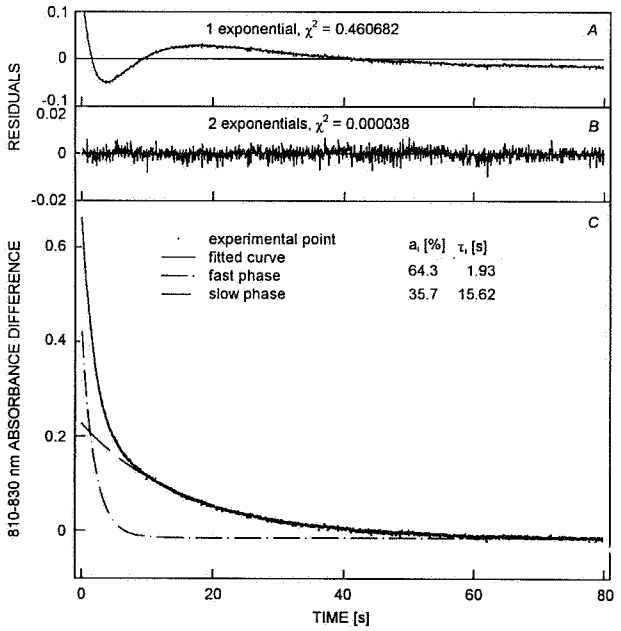

Fig. 2. Reduction kinetics of $P700^+$ subsequent to a 60-s FR irradiation of an intact tobacco leaf that had dark-adapted for 24 min as described in Fig. 1*A*, illustrating the fitting procedures and the de-convolution with the best fit. *A, B*: Residual plots of the fitting of experimental data to mono- and bi-exponential model, respectively. *C*: De-convolution of the fitted bi-exponential curve, showing the corresponding individual contributions of the two kinetic components, with their vertical origins at a_0.

the present experiment excited mainly PS1, and drove cyclic electron flow around it. The imbalance between the electron flow out of PS1 and the electron supply from intersystem carriers caused an accumulation of oxidised P700, resulting in an increase in 810-830 nm absorbance difference. Upon the turning off of FR irradiation, the pool of $P700^+$ was reduced progressively by electrons from cyclic electron flow *via* intersystem electron carriers, which could bring about a decay of 810-830 nm absorbance difference. The decaying phases of the curves in Fig. 1 were expanded and analysed in Figs. 2 and 3. The highly improved signal/noise ratio of the signal makes it possible to analyse the relaxation kinetics accurately.

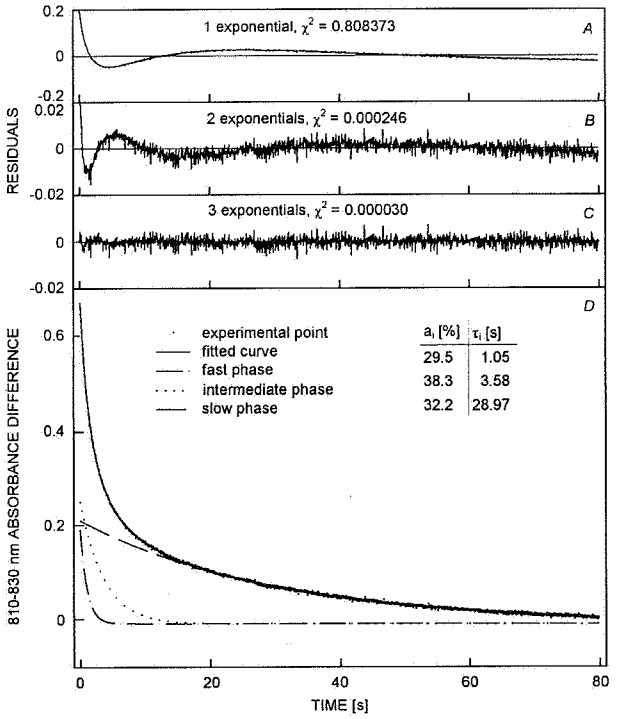

Fig. 3. Reduction kinetics of $P700^+$ as in Fig. 2, except that the tobacco leaf had dark-adapted for 3.31 h, as described in Fig. 1*B*, illustrating the fitting procedures and the de-convolution with the best fit. *A, B, C*: Residual plots of the fitting of experimental data to mono-, bi-, and tri-exponential model, respectively. *D*: De-convolution of the fitted tri-exponential curve, showing the corresponding individual contributions of the three kinetic components, with their vertical origins at a_0.

The decay kinetics of 810-830 nm absorbance difference after the termination of FR irradiation in the intact tobacco leaf dark-adapted for 24 min was deconvoluted distinctively into two exponential components with half-times of about 1.93 and 15.62 s (Fig. 2). Inclusion of a third exponential component did not improve the quality of fit. In contrast, when the dark-adaptation period of the leaf was extended to 3.31 h, the number of exponential decaying components increased to three, with half-times of about 1.03, 3.58, and 28.97 s (Fig. 3).

Extensive investigation of the effects of dark adaptation is shown in Fig. 4, where the half-times and magnitudes of the exponentially decaying components are represented as functions of dark-adaptation period. After short-term dark adaptation, only two exponential decaying phases were resolved from the dark relaxation kinetics. When dark-adaptation period was extended to 40 min, a new exponential decaying component appeared, with a half-time intermediate between those of the fast and slow ones. Meanwhile, the values of half-times, especially that of the slow phase, increased with the prolongation of dark-adaptation period and approached a stable level. The magnitude of the slow phase is quite stable, while that of the fast phase changes complementarily with the intermediate phase.

In Fig. 4*C*, the relative magnitudes of the fast and the slow component are plotted against that of the intermediate one, where the former decreased linearly,

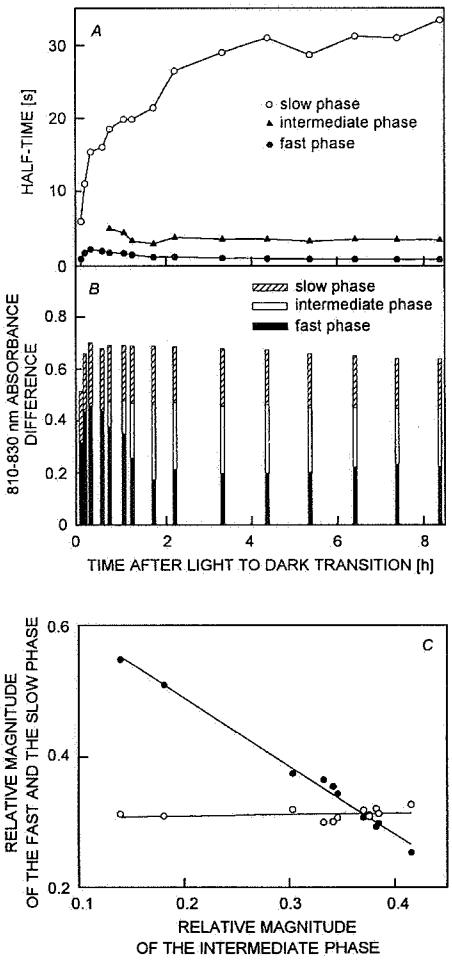

Fig. 4. Influence of dark-adaptation duration on the half-time (*A*) and magnitude (*B*) of the exponential components characterising the $P700^+$ reduction kinetics of tobacco leaf after FR irradiation. The correlation between the relative magnitude of the intermediate phase and those of the other two phases is shown in *C*. The leaf had been irradiated [halogen lamp, 1 000 μmol(photon) m^{-2} s^{-1}] for 15 min before dark-adaptation.

while the latter showed little change. The sum of magnitudes, represented by the height of the sectioned bars in Fig. 4*B*, reflected the steady state level of $P700^+$ induced by FR.

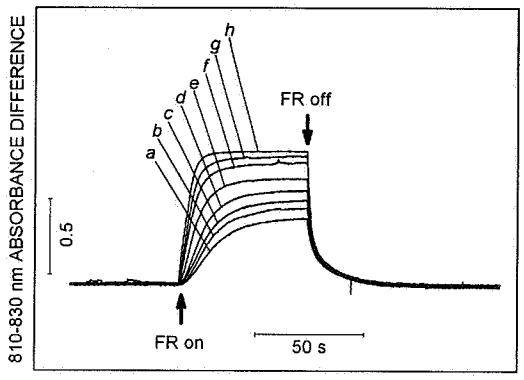

Fig. 5. Irradiance dependence of FR-induced redox kinetics of P700 in intact tobacco leaf. The FR irradiances in *a*, *b*, *c*, *d*, *e*, *f*, *g*, and *h* were 0.82, 1.03, 1.25, 1.56, 2.14, 3.20, 4.30, and 7.30 μmol(photon) m^{-2} s^{-1}, respectively. The leaf had dark-adapted for 1.5 h.

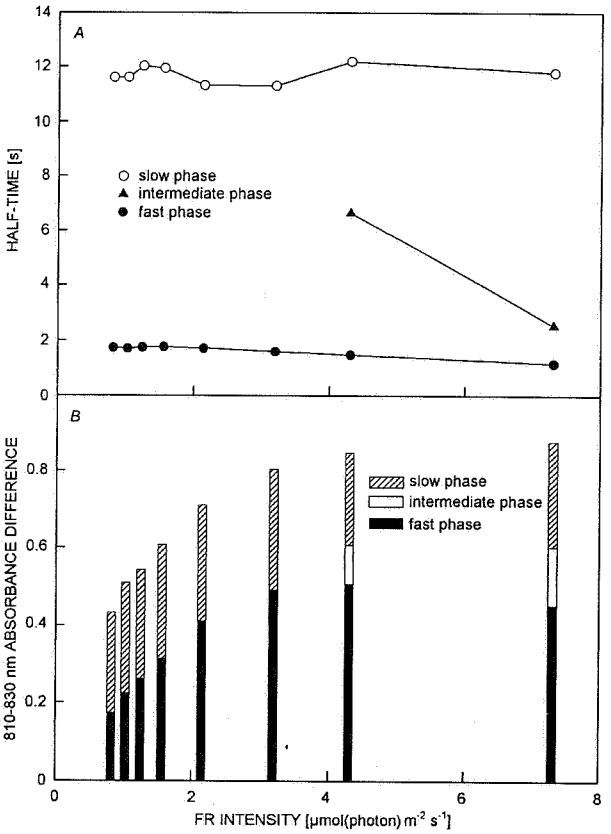

Fig. 6. Influence of FR irradiance on the half-time (*A*) and magnitude (*B*) of the exponential components characterising the $P700^+$ reduction kinetics of the tobacco leaf after FR irradiation as described in Fig. 5.

Under irradiance-limited condition, both the rate and the extent of FR-induced increase in 810-830 nm absorbance difference were strongly influenced by FR irradiance (Fig. 5). Kinetic parameters of the post-irradiation relaxation in the absorbance difference are shown in Fig. 6. At lower FR irradiances, only two exponentially decaying components were resolved. At higher FR irradiances, an intermediate component appeared. In comparison with those of the fast and the slow phases, the half-time of the intermediate phase decreased considerably with the increase of FR irradiance (Fig. 6*A*). The magnitude plot in Fig. 6*B* showed that the irradiance dependence of the extent in FR-induced P700 oxidation arose mainly from the irradiance response of the fast decaying phase.

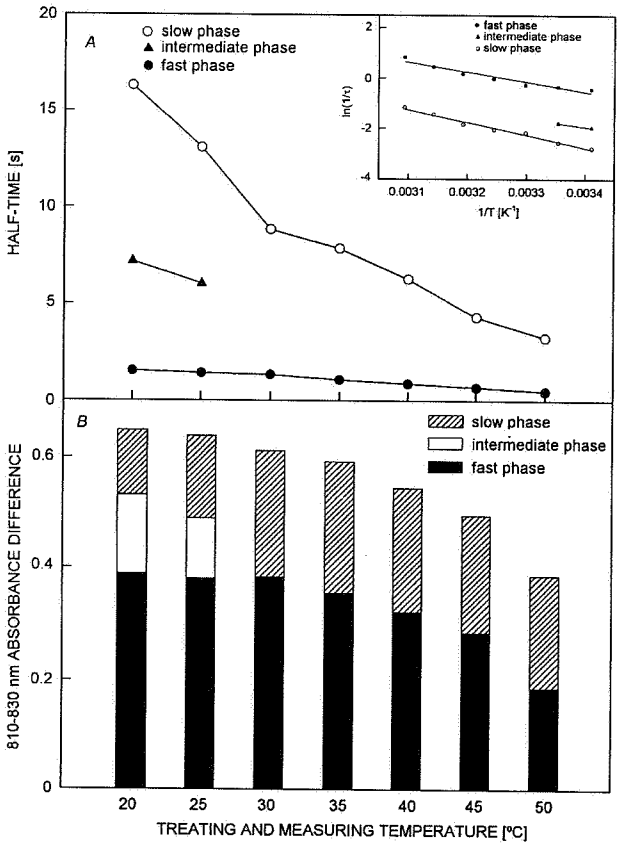

Fig. 7. Temperature-dependence of the half-time (*A*) and magnitude (*B*) of the exponential components characterising the $P700^+$ reduction kinetics after FR irradiation in tobacco leaf. The *inset* in *A* is the Arrhenius plot of the reciprocal of the half-times. The leaf had been exposed to the indicated temperatures for 15 min before measurement, which was carried out at the same temperature as treatment.

The dependence upon temperature from 20 to 55 °C of the kinetics of $P700^+$ re-reduction is depicted in Fig. 7. Higher temperatures caused a decrease in the extent of FR-induced absorption changes and an acceleration

of $P700^+$ reduction after FR irradiation. Elevated temperatures (Fig. 7*A*) accelerated relaxation of both the fast and the slow phases, as well as that of the intermediate phase, which disappeared at higher temperatures. The activation energy of the fast phase and that of the slow phase, as represented by the slopes of the Arrhenius plots in Fig. 7*A*, were similar. Magnitude plot in Fig. 7*B* reveals that the decrease in the extent of P700 redox change at higher temperatures can be ascribed mainly to the thermal sensitivity of the fast phase.

Discussion

The underlying mechanism of multi-phasic kinetics of $P700^+$ reduction after irradiance-excitation has not yet been elucidated. According to Bukhov *et al.* (1999), the biphasic reduction kinetics of $P700^+$ after FR irradiation might correspond to two electron donor systems, *i.e.*, a reduced electron carrier in the cyclic electron transport pathway capable of fast electron donation, perhaps ferredoxin, and NADPH that serves as a slow donor, or to the existence of two different pools of PS1 located in different domains of chloroplast membranes. Here we take the latter explanation as a working hypothesis.

Thylakoid membranes of higher plants can be divided into three main domains according to their biochemical composition and functions: the stroma lamellae, the grana margins, and the grana core (Albertsson *et al.* 1991). PS1 from different domains differs in antenna size (Andreasson *et al.* 1988), electron transport properties (Wollenberger *et al.* 1995) as well as the density of PS1 distribution *per se*, which is extremely low in the central appressed domain of the grana (Albertsson 1995). Distinctness of cytochrome *f* in these three domains has also been observed (Albertsson *et al.* 1991). The heterogeneity of both PS1 and cytochrome *f*, and other, if any, electron carriers involved in PS1-dependent cyclic electron transport may result in the multiphase kinetics of $P700^+$ reduction after FR oxidation.

Following de-excitation, $P700^+$ traps electrons from reduced intersystem electron carriers, and ultimately from stromal reductants. Each kinetic component of $P700^+$ reduction, as indicated by the relaxation of 810-830 nm absorbance difference, may correspond to the rate-limiting step of electron supply to $P700^+$ located in one of the three thylakoid domains listed above. Since the magnitude of the rates of electron transfer within the intersystem chain is far beyond the time resolution of $P700^+$ reduction kinetics observed in the present experiments, it is unlikely that the rate-limiting step lies in thylakoid membrane. The entry of electrons from stromal reductants into intersystem electron carriers is mediated either by NAD(P)H dehydrogenase (NDH) or sequentially by ferredoxin-$NADP^+$ reductase (FNR) and ferredoxin-plastoquinone reductase (FQR) (Bendall and Manasse 1995, Endo *et al.* 1997). Both FNR and the hydrophilic part of NDH are exposed to stroma. Ferredoxin and NADPH, as the member of electron transport chain and the end product of linear electron transport, respectively, are also thermodynamically equilibrated with a large number of stromal reductants (Asada *et al.* 1992, 1998). It seems likely that the rate-limiting step of $P700^+$ dark reduction lies in redox reactions in stroma. Although we have not found documented evidence, there might be regional heterogeneity of stroma matrix with respect to chemical and physical properties among regions adjacent to the stroma lamellae, the grana margins, and the grana core. This may lead to a heterogeneity in the behaviour of electron transfer from stromal reductants into the intersystem chain, as reflected by the multi-phasic kinetics of $P700^+$ re-reduction in the dark.

The effect of dark adaptation on $P700^+$ reduction kinetics may be associated with the reversible conformational changes of thylakoid membranes induced by actinic radiation. Under actinic irradiation, some LHC2s become phosphorylated and dissociated from PS2, move away from PS2, and supply excitation energy to PS1 (Howarth *et al.* 1982, Kyle *et al.* 1983, 1984, Simpson 1983). Light-induced redistribution of cytochrome *bf* has also been reported (Homel *et al.* 2000). During dark-adaptation, the inverse process occurred, which may be reflected by $P700^+$ reduction kinetics (Fig. 4). Since the proportion of the fast kinetic component decreased linearly with the increase in that of the intermediate one (Fig. 4*C*), the appearance of the intermediate phase may be caused by the splitting of the fast phase. This indicates the conformational change of thylakoid membrane during the restoration of light-induced state transition. The depression of the extent of FR-induced P700 oxidation at the early stage of dark-adaptation (Fig. 4*B*) can be explained as the dark relaxation of reducing equivalents accumulated during actinic irradiation (Cornic *et al.* 2000). Strong irradiance can cause an over-reduction of stromal redox components, and thus a decrease in P700 oxidation during subsequent FR irradiation (Endo *et al.* 1999).

As reported by Andreasson *et al.* (1988), the PS1 and PS2 in stacked thylakoid membranes have larger functional antenna sizes than the corresponding PS1 and PS2 in the stroma membranes. This suggests that photosystems in grana can allow effective electron transport both at low and high irradiances, while the stroma-membrane photosystems work mainly at high irradiances as a supplement to the grana systems. We found (Fig. 6*B*) that under irradiance-limiting condition the FR dependence of the extent of P700 oxidation can be attributed mainly to the light-responsibility of the fast phase of $P700^+$ reduction kinetics after FR irradiation, indicating that the fast

phase corresponds to the PS1 located in grana domain.

There is an extensive literature on the thermal denaturation of photosynthetic apparatus. In comparison with PS2, PS1 is more tolerant to heat stress (Yamashita and Butler 1968, Boucher and Carpentier 1993, Havaux 1996, Bukhov *et al.* 1999). There are documented circumstances where the dark-reduction of intersystem electron carriers was enhanced at higher temperatures (Havaux 1996, Bukhov *et al.* 1999). Within the range of temperature employed in the present study, all the kinetic components of post-irradiation $P700^+$ reduction were accelerated at elevated temperatures (Fig. 7*A*), indicating the enhancement of electron transfer from stromal reductants into the intersystem chain, especially the activation of stroma-located reactions. The decrease in extent of FR-induced P700 oxidation at higher temperatures (Fig. 7*B*) can probably be attributed to the thermal enhancement of electron supply from stroma, which caused a decrease in the steady state level of $P700^+$ under FR irradiation. The disappearance of the intermediate kinetic component at higher temperatures might be due to some heat-induced structural changes in thylakoid membranes (Sundby *et al.* 1986).

We observed here for the first time the variation in the number of kinetic components of $P700^+$ dark reduction in response to environmental changes. The attribution of the multi-phasic kinetics to the heterogeneity of PS1 activity is just a tentative interpretation. More convincing evidence is needed to substantiate this hypothesis.

References

Albertsson, P.- Å.: The structure and function of the chloroplast photosynthetic membrane – a model for the domain organization. – Photosynth. Res. **46**: 141-149, 1995.

Albertsson, P.-Å., Andreasson, E., Svensson, P., Yu, S.-G.: Localization of cytochrome *f* in the thylakoid membrane: evidence for multiple domains. – Biochim. biophys. Acta **1098**: 90-94, 1991.

Andreasson, E., Svensson, P., Weibull, C., Albertsson, P.-Å.: Separation and characterization of stroma and grana membranes – evidence for heterogeneity in antenna size of both Photosystem I and Photosystem II. – Biochim. biophys. Acta **936**: 339-350, 1988.

Asada, K., Endo, T., Mano, J., Miyake, C.: Molecular mechanism for relaxation of and protection from light stress. – In: Satoh, K., Murata, N. (ed.): Stress Reponses of Photosynthetic Organisms. Pp. 37-52. Elsevier, Tokyo – Amsterdam 1998.

Asada, K., Heber, U., Schreiber, U.: Pool size of electrons that can be donated to $P700^+$, as determined in intact leaves: Donation to $P700^+$ from stromal components via the intersystem chain. – Plant Cell Physiol. **34**: 35-50, 1992.

Bendall, D.S., Manasse, R.S.: Cyclic phosphorylation and electron transport. – Biochim. biophys. Acta **1229**: 23-38, 1995.

Boucher, N., Carpentier, R.: Heat-stress stimulation of oxygen uptake by Photosystem I involves the reduction of superoxide radicals by specific electron donors. – Photosynth. Res. **35**: 213-218, 1993.

Bukhov, N.G., Wiese, C., Neimanis, S., Heber, U.: Heat sensitivity of chloroplasts and leaves: Leakage of protons from thylakoids and reversible activation of cyclic electron transport. – Photosynth. Res. **59**: 81-93, 1999.

Cornic, G., Bukhov, N.G., Wiese, C., Bligny, R., Heber, U.: Flexible coupling between light-dependent electron and vectorial proton transport in illuminated leaves of C3 plants. Role of photosystem I-dependent proton pumping. – Planta **210**: 468-477, 2000.

Endo, T., Mi, H., Shikanai, T., Asada, K.: Donation of electrons to plastoquinone by NAD(P)H dehydrogenase and by ferredoxin-quinone reductase in spinach chloroplasts. – Plant Cell Physiol. **38**: 1272-1277, 1997.

Endo, T., Shikanai, T., Takabayushi, A., Asada, K., Sato, F.: The role of chloroplastic NAD(P)H dehydrogenase in photoprotection. – FEBS Lett. **457**: 5-8, 1999.

Harbinson, J., Woodward, F.I.: The use of light-induced absorbance changes at 820 nm to monitor the oxidation state of P-700 in leaves. – Plant Cell Environ. **10**: 131-140, 1987.

Havaux, M.: Short-term responses of Photosystem I to heat stress. Induction of a PS II-independent electron transport through PS I fed by stromal components. – Photosynth. Res. **47**: 85-97, 1996.

Homel, P., Olive, J., Pierre, Y., Wollman, F.A., de Vitry, C.: A new subunit of cytochrome b_6f complex undergoes reversible phosphorylation upon state transition. – J. biol. Chem. **275**: 17072-17079, 2000.

Howarth, P., Kyle, D.J., Horton, P., Arntzen, C.J.: Chloroplast membrane protein phosphorylation. – Photochem. Photobiol. **36**: 743-748, 1982.

Jin, M.-X., Mi, H., Ye, J.-Y., Shen, Y.-G.: Mathematical analysis of post-illumination transient increase in chlorophyll fluorescence and its dependence upon illumination duration in maize leaves. – Acta phytophysiol. sin. **26**: 219-226, 2000.

Klughammer, C., Schreiber, U.: Analysis of light-induced absorbance changes in the near-infrared spectral region. I. Characterization of various components in isolated chloroplasts. – Z. Naturforsch. **46c**: 233-244, 1991.

Klughammer, C., Schreiber, U.: Measuring P700 absorbance changes in the near infrared spectral region with a dual wavelength pulse modulation system. – In: Garab, G. (ed.): Photosynthesis: Mechanisms and Effects. Vol. V. Pp. 4357-4360. Kluwer Academic Publ., Dordrecht – Boston – London 1998.

Kyle, D.J., Kuang, T.-Y., Watson, J.L., Arntzen, C.J.: Movement of a sub-population of the light harvesting complex (LHC_{II}) from grana to stroma lamellae as a consequence of its phosphorylation. – Biochim. biophys. Acta **765**: 89-96, 1984.

Kyle, D.J., Staehelin, L.A., Arntzen, C.J.: Lateral mobility of the light-harvesting complex in chloroplast membrane controls excitation energy distribution in higher plants. – Arch. Biochem. Biophys. **222**: 527-541, 1983.

Marquardt, D.W.: An algorithm for least-squares estimation of nonlinear parameters. – J. Soc. ind. appl. Math. **11**: 431-441, 1963.

Schreiber, U., Klughammer, C., Neubauer, C.: Measuring P700 absorbance changes around 830 nm with a new type of pulse modulation system. – Z. Naturforsch. **43c**: 686-698, 1988.

Simpson, D.J.: Freeze-fracture studies on barley plastid membranes. VII. Structural changes associated with phosphorylation of the light-harvesting complex. – Biochim. biophys. Acta **725**: 113-120, 1983.

Sundby, C., Melis, A., Mäenpää, P., Andersson, B.: Temperature-dependent changes in the antenna size of Photosystem II. Reversible conversion of Photosystem II_α to Photosystem II_β. – Biochim. biophys. Acta **851**: 475-483, 1986.

Wollenberger, L., Weibull, C., Albertsson, P.-Å.: Further characterization of the chloroplast grana margins: the non-detergent preparation of granal photosystem I cannot reduce ferredoxin in the absence of $NADP^+$ reduction. – Biochim. biophys. Acta **1230**: 10-22, 1995.

Yamashita, T., Butler, W.L.: Inhibition of chloroplasts by UV-irradiation and heat-treatment. – Plant Physiol. **43**: 2037-2040, 1968.